JOURNAL OF VIROLOGY, Aug. 2000, p. 7562–7567 Vol. 74, No. 16
0022-538X/00/$04.00+0

Using Chimeric Hypoviruses To Fine-Tune the Interaction between a Pathogenic Fungus and Its Plant Host

BAOSHAN CHEN,[1] LYNN M. GELETKA, AND DONALD L. NUSS*

Center for Agricultural Biotechnology, University of Maryland Biotechnology Institute, College Park, Maryland 20742-4450

Received 13 April 2000/Accepted 18 May 2000

Infectious cDNA clones of mild (CHV1-Euro7) and severe (CHV1-EP713) hypovirus strains responsible for virulence attenuation (hypovirulence) of the chestnut blight fungus *Cryphonectria parasitica* were used to construct viable chimeric viruses. Differences in virus-mediated alterations of fungal colony morphology, growth rate, and canker morphology were mapped to a region of open reading frame B extending from nucleotides 2,363 to 9,904. By swapping domains within this region, it was possible to generate chimeric hypovirus-infected *C. parasitica* isolates that exhibited a spectrum of defined colony and canker morphologies. Several severe strain traits were observed to be dominant. It was also possible to uncouple the severe strain traits of small canker size and suppression of asexual sporulation. For example, fungal isolates infected with a chimera containing nucleotides 2363 through 5310 from CHV1-Euro7 in a CHV1-713 background formed small cankers that were similar in size to that caused by CHV1-EP713-infected isolates but with the capacity for producing asexual spores at levels approaching that observed for fungal isolates infected with the mild strain. These results demonstrate that hypoviruses can be engineered to fine-tune the interaction between a pathogenic fungus and its plant host. The identification of specific hypovirus domains that differentially contribute to canker morphology and sporulation levels also provides considerable utility for continuing efforts to enhance biological control potential by balancing hypovirulence and ecological fitness.

An underlying tenet of contemporary plant biology is that an increased understanding of how plants and microbes communicate will lead to new strategies for preventing pathogenic interactions. In this regard, the phenomenon of hypovirulence, in which mycoviruses attenuate fungal virulence, is providing insights into mechanisms that regulate interactions between fungal pathogens and plant hosts. For example, efforts designed to understand how viruses of the family *Hypoviridae* reduce virulence of the chestnut blight fungus *Cryphonectria parasitica* have revealed a crucial role for G-protein signal transduction in a wide range of vital fungal physiological processes, including fungal pathogenesis (7, 10, 12, 18, 19). It has been proposed that hypoviruses compromise the ability of the invading fungus to respond appropriately to events at the fungus-plant interface by disrupting fungal signaling pathways, thereby impeding penetration, canker expansion, and fungal reproduction (reviewed in reference 23). Interest in virulence-attenuating mycoviruses has also been stimulated by several reports of partial or effective field control of plant-pathogenic fungi (1, 3, 4, 13, 17, 22, 28).

The concept of engineering mycoviruses for purposes of manipulating fungal pathogens was significantly advanced by the development of an infectious cDNA copy of the prototypic hypovirus CHV1-EP713 (9). The potential for practical and fundamental applications of this group of viruses was further enhanced by the recent construction of an infectious cDNA clone of a second hypovirus, CHV1-Euro7 (8). By analogy with plant viruses, CHV1-EP713 and CHV1-Euro7 can be viewed as severe and mild hypovirus strains, respectively. CHV1-EP713-infected *C. parasitica* strains are severely compromised in the ability to expand on chestnut tissue and form small, superficial cankers with few, if any, asexual spore-forming fruiting bodies (stromal pustules). In contrast, CHV1-Euro7-infected strains exhibit an aggressive colonization of chestnut tissue early after inoculation. The resulting cankers, which attain a size three- to fourfold larger than those produced by CHV1-EP713-infected strains before expansion abruptly ceases, are characterized by distinctively ridged margins and the formation of a significant level of spore-forming pustules covering the canker face.

We now report the construction and characterization of a collection of stable chimeric recombinant viruses from the CHV1-EP713 and CHV1-Euro7 infectious cDNAs. The results clearly demonstrate that hypoviruses can be engineered to fine-tune the interaction between a fungal pathogen and its plant host and illustrate the utility of this approach for mapping the contribution of specific regions of the hypovirus genome to virus-mediated alterations of fungal phenotype and virulence. The implications of these results for enhanced biological control potential are also discussed.

MATERIALS AND METHODS

Fungal isolates, growth conditions, and phenotypic measurements. Hypovirus-free *C. parasitica* isolate EP155 (ATCC 38755) and corresponding hypovirus-transfected isolates were maintained on potato dextrose agar (PDA; Difco, Detroit, Mich.) on the laboratory benchtop at 22 to 24°C and characterized as previously described (14). To ensure consistency for phenotypic measurements and observations, parallel inoculation cultures were initiated by transfer of mycelial plugs directly from transfection regeneration plates to PDA (8). Virulence assays (five duplicates for each treatment) were performed with dormant American chestnut tree stems as previously described (9, 16).

Construction of chimeric hypoviruses. Prototypic hypovirus CHV1-EP713 was purified from the hypovirulent *C. parasitica* isolate EP713 (ATCC 52571), which was obtained via anastomosis-mediated transmission of the hypovirus from the French hypovirulent isolate EP113 into the North American isolate EP155 (2). A full-length infectious cDNA clone of CHV1-EP713 RNA, plasmid pLDST, was constructed by Choi and Nuss (9). Chen and Nuss (8) recently reported construction of a full-length infectious cDNA clone, pET7, of a second hypovirus,

* Corresponding author. Mailing address: Center for Agricultural Biotechnology, University of Maryland Biotechnology Institute, Plant Sciences Bldg., Rm. 5115C, College Park, MD 20742-4450. Phone: (301) 405-0334. Fax: (301) 314-9075. E-mail: nuss@umbi.umd.edu.

† Present address: Biotechnology Research Center, Guangxi University, Nanning, Guangxi 530005, People's Republic of China.

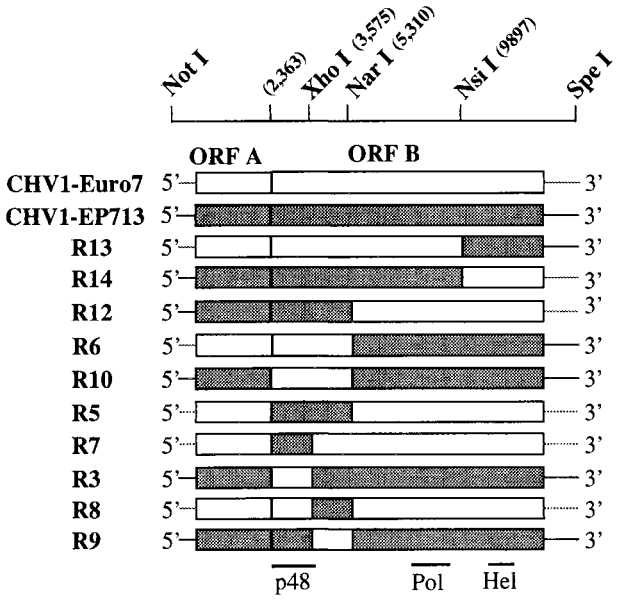

FIG. 1. Schematic diagram of parental and chimeric hypoviruses used in this study. The position of restriction sites used to generate chimeric viruses from CHV1-Euro7 (coding regions are indicated as white boxes, and noncoding regions are indicated as gray lines) and CHV1-EP713 (coding regions are presented as gray boxes, and noncoding regions are presented as black lines) are indicated at the top. The unique *Not*I site fused to a minimal T7 polymerase promoter was introduced immediately upstream of the viral sequence in both parental cDNAs to facilitate swapping of the 5′ portions and in vitro transcription. Similarly, the *Spe*I site was introduced immediately after the viral poly(A) tail to allow linearization of the plasmid in preparation for in vitro transcription and to aid in swapping of the 3′ portions of the viruses. The CHV1-Euro7 map positions for the three restriction sites common to the two viruses are nt 3575 for *Xho*I, nt 5310 for *Nar*I, and nt 9898 for *Nsi*I. Since CHV1-Euro7 is 11 nt shorter than CHV1-EP713 (12,701 nt versus 12,712 nt), the map position numbering for the two viruses differs slightly (8). The approximate positions of the p48, putative RNA-dependent RNA polymerase (Pol), and putative RNA helicase (Hel) coding domains are indicated at the bottom of the figure (20, 25).

CHV1-Euro7. CHV1-Euro7 RNA was purified from *C. parasitica* isolate Euro7 (ATCC 66021) recovered in 1978 by William MacDonald (West Virginia University) from a superficial canker on a European chestnut coppice sprout approximately 30 km north of Florence, Italy. All laboratory virus infections were established by transfection of virus-free *C. parasitica* EP155 with in vitro-synthesized viral transcripts as described previously (6, 8).

To facilitate construction of chimeric viruses, a multistep procedure was designed to move the full-length parental hypovirus cDNAs into a modified pPCRScript AmpSK(+) (Stratagene, La Jolla, Calif.) plasmid vector. The 5′ terminus of the viral cDNA was immediately preceded by a T7 bacteriophage polymerase promoter fused upstream to a unique *Not*I restriction site. The 3′ terminus of the viral cDNA was followed by a unique *Spe*I site used to linearize the plasmid for in vitro transcription (Fig. 1). A block of restriction sites within the original multiple cloning site extending from *Eco*RI through *Kpn*I was deleted to simplify subsequent cloning procedures. Construction of chimeric viruses relied on several restriction sites that were conserved in the two hypovirus coding domains: an *Xho*I site at map position 3575, a *Nar*I site at position 5310, and an *Nsi*I site at position 9897 (CHV1-Euro7 map coordinates [8] are listed) as indicated in Fig. 1. A description of detailed cloning steps is available from D.L.N. upon request.

Analysis of hypovirus dsRNA. Viral double-stranded RNA (dsRNA) was extracted from 5-day-old infected mycelia cultured in liquid EP Complete Medium (24) according to the protocol of Hillman et al. (14). Partially purified viral dsRNA preparations were treated with S1 nuclease (5 U) to digest single-stranded RNA (6). The quality and quantity of each preparation was examined by agarose (0.8%) gel electrophoresis (14).

RESULTS

Construction of chimeric hypoviruses. Hypoviruses of the genus CHV1 contain two contiguous open reading frames (ORFs), ORF A and ORF B (15). ORF A encodes two polypeptides, p29 and p40, that are released from polyprotein p69 by an autocatalytic event mediated by the papain-like protease domain within p29 (25). Expression of ORF B, which contains putative RNA-dependent RNA polymerase and RNA helicase coding motifs, also involves an autoproteolytic event in which a second papain-like protease, p48, is released from the N-terminal portion of the encoded polyprotein (27).

Chen and Nuss (8) recently demonstrated that the two ORFs of CHV1-EP713 and CHV1-Euro7 could be interchanged without negatively affecting viral replication. It was concluded from that study that the differences in symptoms caused by the two viruses were encoded primarily by domains within ORF B, while the ORF A portions appeared to make similar contributions to the overall level of virus-mediated alteration of fungal phenotype. Although these initial chimeras were replication competent and genetically stable, it was unclear whether the swapping of other domains, e.g., portions within ORF B, would be tolerated. An additional potential complication in constructing stable chimeras is the paucity of information concerning the processing of the ORF B-encoded polyprotein. Consequently, domain swaps were defined in this study by the availability of unique restriction sites within ORF B that were common to the two viruses: *Xho*I at CHV1-Euro7 map position 3575, *Nar*I at map position 5310, and *Nsi*I at map position 9897 (Fig. 1). The *Xho*I site is located just 41 nucleotides (nt) 5′ of the p48 cleavage site. Thus, a chimeric virus constructed with this site would encode a chimeric p48 protein that contained 403 N-terminal amino acids from one parent and only 14 C-terminal amino acids from the other parent. The *Nar*I site lies 1,649 nt (564 codons) downstream of the p48 cleavage site in a region of the ORF B polyprotein that has not been assigned any known function. The *Nsi*I site lies between the putative polymerase and helicase coding domains (20). Thus, chimeric viruses constructed at this site would have a heterologous replication complex consisting of helicase and polymerase domains derived from the two different parental viruses. The collection of chimeric viruses examined in this study are illustrated diagrammatically in Fig. 1.

Influence of chimeric hypovirus infection on fungal phenotype. Transfection of *C. parasitica* with synthetic transcripts of each chimera resulted in a productive infection causing a spectrum of defined virus-induced colony morphologies (Fig. 2, Table 1). CHV1-EP713-infected *C. parasitica* strains grow more slowly than the corresponding virus-free strains on synthetic PDA media. The colonies are characterized by hyphae that penetrate into the media, by irregular margins, and by the general absence of asexual spores. CHV1-Euro7-infected *C. parasitica* strains actually exhibit faster radial growth than the corresponding virus-free strain and produce abundant aerial hyphae and pustules containing viable asexual spores (8). Chimeric viruses constructed at the *Nsi*I site (R13 and R14) had properties similar to the parental viruses from which the region upstream of the *Nsi*I site was derived. That is, chimeric virus R13, composed predominantly of CHV1-Euro7, caused a colony morphology similar to CHV1-Euro7-infected isolates, while the reciprocal chimera R14 caused a colony morphology similar to that caused by CHV1-EP713. Thus, neither the 3′-terminal portion of the ORF B coding domain nor the 3′-noncoding region appears to contribute to differences in the colony morphologies caused by the two parental viruses. This result is similar to that obtained with the previously described chimeric viruses in which the 5′-proximal domains, including the 5′-noncoding region and ORF A, were swapped (8). The combined results suggest that the portion of ORF B responsible for the differences in virus-induced colony morphologies resides between the N terminus (nt 2363) and nt 9897. The fact that chimeras R13 and R14 were infectious also indicates that the

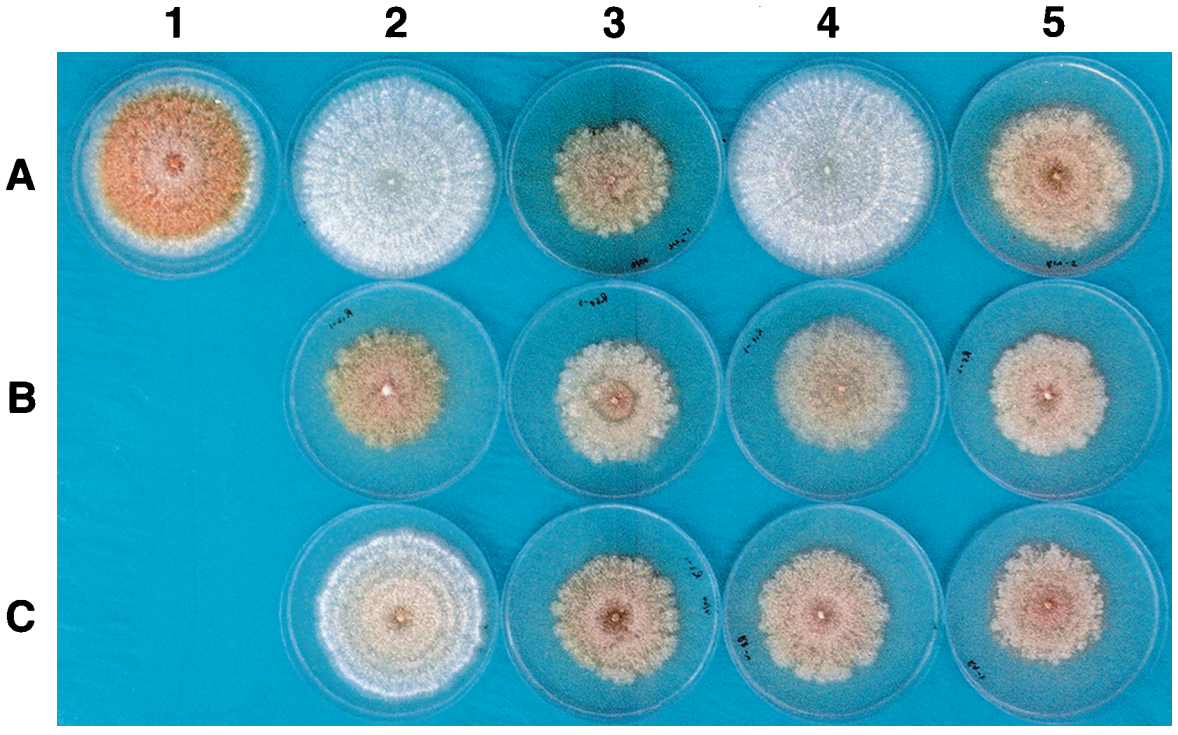

FIG. 2. Colony morphologies on PDA conferred by parental and chimeric hypoviruses. A colony of virus-free *C. parasitica* isolate EP155 is shown at the top left (A1). Colonies transfected with parental viruses CHV1-Euro7 and CHV1-EP713 are shown at coordinates A2 and A3, respectively. Colonies infected with chimeric viruses are shown at the following coordinates: R13, A4; R14, A5; R12, B2; R6, B3; R10, B4; R5, B5; R7, C2; R3, C3; R8, C4; and R9, C5. The photograph was taken on day 7 of culture on PDA.

polymerase and helicase domains of the two viruses are compatible. In this regard, the double-stranded form of each chimeric virus RNA examined in this report accumulated in the fungus to similar levels (Fig. 3), a finding consistent with a similar level of replication competence for each chimera.

The region between nt 2363 and 9897 was further mapped by constructing reciprocal chimeras using the *Xho*I and *Nar*I restriction sites. Relative contributions of the region extending from nt 2363 to 5310 were examined in two configurations: paired with either the homologous or the heterologous ORF A coding domain (Fig. 1). Note that transfection with the reciprocal chimeras R12 and R6 resulted in colony morphologies that were very similar to each other and to that exhibited by CHV1-EP713-infected isolates (Fig. 2, B2 and B3; Table 1). This observation indicates that the severe CHV1-EP713 colony

TABLE 1. Effect of transfection with wild-type and chimeric hypovirus transcripts on fungal radial growth on synthetic medium

Strain	Colony size ± SD (cm^2)[a] at:	
	Day 5	Day 7
EP155	22.2 ± 0.5	47.3 ± 0.9
EP155/CHV1-Euro7	26.6 ± 1.0	51.0 ± 1.1
EP155/CHV1-EP713	11.2 ± 0.8	16.5 ± 0.7
EP155/R13	27.3 ± 1.1	51.8 ± 1.7
EP155/R14	15.4 ± 1.3	24.1 ± 1.7
EP155/R12	11.7 ± 0.7	15.9 ± 1.1
EP155/R6	13.2 ± 0.5	20.3 ± 1.1
EP155/R10	12.1 ± 0.9	21.8 ± 1.9
EP155/R5	11.8 ± 0.6	17.8 ± 1.0
EP155/R7	20.5 ± 1.5	40.0 ± 1.7
EP155/R3	12.7 ± 1.4	17.4 ± 1.2
EP155/R8	13.5 ± 1.5	20.1 ± 1.0
EP155/R9	13.2 ± 0.3	19.5 ± 0.8

[a] Fungal cultures were grown in parallel on PDA in 85-mm-diameter petri dishes under standard laboratory bench conditions (14).

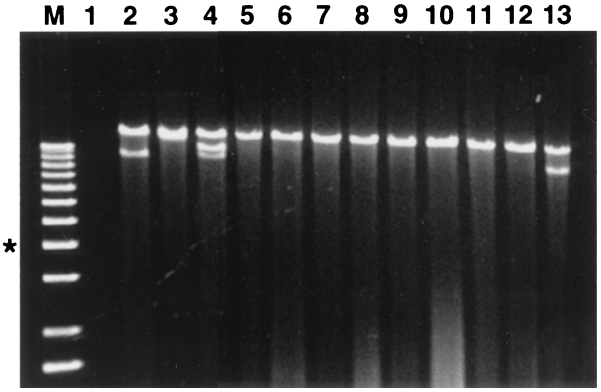

FIG. 3. Agarose gel electrophoretic analysis of dsRNAs recovered from transfected *C. parasitica* isolates. The full-length viral dsRNAs are the slowest-migrating band in each lane. The faster-migrating species observed in lanes 2, 4, and 13 correspond to internally deleted defective viral RNAs previously identified in hypovirus-infected fungal isolates (5, 26). The presence of these defective RNAs has not been associated with any changes in fungal phenotype. Lane M, 200 ng of 1-kb DNA ladder (Gibco BRL) as relative size markers, with an asterisk indicating the position of the 4-kb band. Samples (1 μg) of partially purified viral dsRNA recovered from liquid cultures of individual transfected isolates were treated with S1 nuclease (5 U) and analyzed on 0.8% agarose gels. Lane 1, virus-free isolate EP155; lane 2, CHV1-EP713 transfectant; lane 3, CHV1-Euro7 transfectant; lane 4, R13 transfectant; lane 5, R14 transfectant; lane 6, R12 transfectant; lane 7, R6 transfectant; lane 8, R10 transfectant; lane 9, R5 transfectant; lane 10, R7 transfectant; lane 11, R3 transfectant; lane 12, R8 transfectant; lane 13, R9 transfectant.

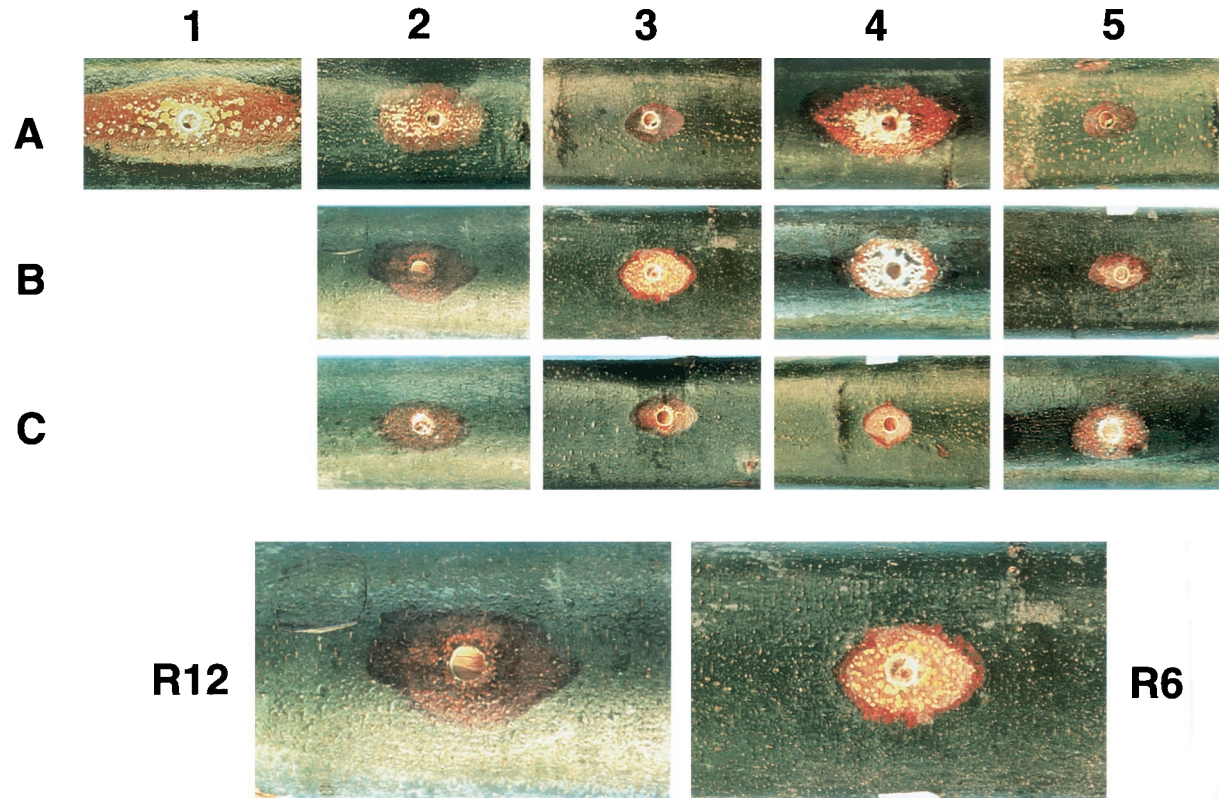

FIG. 4. Representative cankers formed by virus-free and transfected *C. parasitica* isolates. The same coordinate system for strains transfected with chimeric viruses used in Fig. 2 is repeated here: EP155, A1; CHV1-Euro7, A2; CHV1-EP713, A3; R13, A4; R14, A5; R12, B2; R6, B3; R10, B4; R5, B5; R7, C2; R3, C3; R8, C4; and R9, C5. Cankers were photographed 30 days postinoculation. Cankers caused by R12 and R6 transfected isolates are enlarged at the bottom of the figure to illustrate contrast and to allow a closer inspection of the stromal pustules that contain spore-forming bodies, termed pycnidia, and the ridged margins of the canker formed by the R6 transfectant.

morphology phenotype is dominant and that independent determinants of the phenotype reside on either side of the *Nar*I site (nt 5310). Little difference in colony morphology resulted from swapping the ORF A portions of the R12 and R6 chimeras to form R10 and R5 (Fig. 2, B4 and B5). This result is consistent with the previous conclusion that the ORF A domain does not make major contributions to the differences in phenotypic changes caused by the two viruses. However, closer inspection revealed that R5-infected colonies did produce slightly more aerial hyphae than colonies infected with the R12 chimera that differed from the former only in having a heterologous ORF A (data not shown). This subtle difference suggests possible functional interactions between protein products of ORF A and the region from nt 2363 to 5310 of ORF B.

Further dissection of the domain extending from nt 2363 to 5310, using the *Xho*I site, resulted in several interesting observations. Insertion of nt 2363 to 3575 from CHV1-EP713 into the CHV1-Euro7 background, chimera R7, caused a colony morphology intermediate between the two parental phenotypes, while the reciprocal chimera, R3, caused a CHV1-EP713 type of colony (Fig. 2, C2 and C3; Table 1). In contrast to the result observed for R7, insertion of nt 3575 to 5310 from CHV1-EP713 into the CHV1-Euro7 background, R8, caused a severe colony morphology phenotype (Fig. 2, C4). This striking result suggests that the latter region encodes a dominant determinant that is predominantly responsible for the differences in colony morphology observed for the two viruses. However, the fact that the reciprocal chimera, R9, which contained the region from nt 3575 to 5310 from CHV1-Euro7 in a CHV1-EP713 background, and chimera R6, which contained the region from nt 2363 to 5310 from CHV1-Euro7 in the CHV1-EP713 background, also caused a severe colony morphology indicates that regions in CHV1-EP713 flanking nt 3575 to 5319 also make significant contributions to the severe colony morphology.

Influence of chimeric hypovirus infection on fungal-plant host interactions. The collection of chimeric viruses also caused transfected *C. parasitica* strains to produce a spectrum of defined canker morphologies. As illustrated by the representative photographs in Fig. 4 and the quantitative data in Table 2, virus-free *C. parasitica* isolates (Fig. 4, A1) aggressively colonize dormant chestnut stems to produce large cankers that generally continue to expand until a complete girdling of the stem has occurred. The surface of these cankers are densely packed with orange spore-containing stromal pustules that erupt through the bark as expansion proceeds. In contrast, CHV1-EP713-infected fungal isolates (Fig. 4, A3) are severely reduced in the ability to expand on chestnut tissue forming small, superficial cankers that contain few, often no, pustules. CHV1-Euro7-infected fungal isolates (Fig. 4, A2) are quite aggressive in the initial colonization of chestnut tissue but abruptly cease expansion concomitant with the formation of distinctive ridged canker margins suggestive of callus formation. These cankers generally attain a size three- to fourfold larger than those caused by CHV1-EP713-infected isolates and are covered with a significant level of spore-containing pustules (8).

As was observed for colony morphology, cankers formed by fungal isolates infected with chimera R13 were very similar to those caused by isolates infected with CHV1-Euro7, while can-

TABLE 2. Effect of transfection with wild-type and chimeric hypovirus transcripts on canker expansion and production of asexual spore-containing stromal pustules on cankered chestnut tissue

Strain	Canker size ± SD (cm^2)		Stromata/canker[a] ± SD at day 30
	Day 10	Day 30	
EP155	3.1 ± 0.9	23.8 ± 7.8	130.0 ± 11.2
EP155/CHV1-Euro7	2.3 ± 0.2	3.7 ± 0.5	59.6 ± 11.7
EP155/CHV1-EP713	0.9 ± 0.1	1.1 ± 0.3	6.6 ± 5.3
EP155/R13	2.6 ± 0.5	4.5 ± 1.1	68.6 ± 20.1
EP155/R14	0.9 ± 0.2	1.2 ± 0.2	1.8 ± 2.2
EP155/R12	1.1 ± 0.3	1.4 ± 0.3	13.6 ± 7.7
EP155/R6	1.3 ± 0.1	1.5 ± 0.2	33.2 ± 12.6
EP155/R10	1.1 ± 0.2	1.7 ± 0.3	38.4 ± 22.1
EP155/R5	1.1 ± 0.3	1.2 ± 0.3	14.8 ± 6.6
EP155/R7	1.8 ± 0.2	1.9 ± 0.3	7.2 ± 5.0
EP155/R3	1.1 ± 0.2	1.2 ± 0.2	28.2 ± 6.6
EP155/R8	1.1 ± 0.3	1.4 ± 0.4	31.8 ± 15.4
EP155/R9	1.4 ± 0.3	1.6 ± 0.3	47.6 ± 19.9

[a] The number of stromata (stromal pustules) per canker was determined only at day 30.

kers formed by R14-infected isolates were similar to those formed by isolates infected with CHV1-EP713 (Fig. 4, A4 and A5; Table 2). Surprisingly, the similarities between colony and canker morphologies did not extend to the reciprocal chimera pair R12 and R6 (Fig. 4, B2 and B3). While both chimeras caused the formation of small cankers similar in size to the CHV1-EP713 morphology, cankers produced by the R6-infected chimera contained a significant number of pustules and a degree of ridged margins characteristic of CHV1-Euro7 induced cankers (see the enlarged cankers at the bottom of Fig. 4). Thus, the difference exhibited by CHV1-EP713 and CHV1-Euro7 in repressing conidiation on cankers maps to the region extending from nt 2363 to 5310, while determinants responsible for differences in canker size for the two viruses reside on both sides of the *Nar*I site. Swapping of the ORF A portions of chimeras R12 and R6 to form R10 and R5 (Fig. 4, B4 and B5, respectively) had no observable influence on canker morphology.

The insertion of nt 2363 to 3575 from CHV1-EP713 into the CHV1-Euro7 background (R7) significantly reduced both canker size and pustule formation relative to that observed for CHV1-Euro7-infected isolates (Fig. 4, C2, Table 2). This result suggests that the CHV1-EP713 p48 coding domain contains a dominant determinant for suppression of pustule formation. However, the fact that the insertion of the comparable region from CHV1-Euro7 into a CHV1-EP713 background to form R3 (Fig. 4, C3) failed to increase canker size or restore pustule formation to the full level observed for CHV1-Euro7-infected isolates indicates that domains flanking p48 also contribute to reduced canker size and suppression of pustule formation.

Evidence for a potential functional interaction between CHV1-EP713 p48 and proteins encoded within the region from nt 3575 to 5310 was provided by examining the reciprocal chimeras R8 and R9. Insertion of nt 3575 to 5310 from CHV1-EP713 into the CHV1-Euro7 background (R8) resulted in small cankers with intermediate levels of pustule production, a result similar to that observed for isolates infected with chimeras R6 and R10 (Fig. 4, C4; Table 2). Thus, the CHV1-EP713 region from nt 3575 to 5310, while reducing canker size, does not appear by itself to cause a significant reduction in pustule formation. Interestingly, replacing this region in a CHV1-EP713 background with the CHV1-Euro7 homolog, chimera R9, resulted in significantly higher levels of pustule formation (Fig. 4, C5). This result suggests that CHV1-EP713 p48-mediated suppression of pustule formation depends on some sort of interaction with proteins encoded within the CHV1-EP713 region from nt 3575 to 5310.

DISCUSSION

The ability to alter, in a defined manner, *C. parasitica* phenotypic traits, including canker morphology, by simply swapping domains of a severe and a mild hypovirus strain has both fundamental and practical implications. In many respects, the engineering of mycoviruses for the control of pathogenic fungi is analogous to the use of animal viruses in contemporary gene therapy. The goal in both cases is to stably alter host phenotype in a predictable and efficacious manner.

Chen and Nuss (8) predicted that the mapping of determinants responsible for differences in symptoms caused by severe and mild hypovirus strains would ultimately lead to the identification of the viral domains responsible for the underlying symptoms. The results presented here provide a first approximation of the number and location of such determinants. It was somewhat surprising that chimeras which contained CHV1-EP713 ORF B sequences extending either from nt 2363 to 5310 (R12 and R5) or from nt 5310 to 9897 (R6 and R10) all conferred a CHV1-EP713-like colony morphology. This observation supports the view that CHV1-EP713 ORF B encodes multiple independent dominant determinants of colony morphology located on either side of the *Nar*I site at position 5310. A major determinant upstream of the *Nar*I site was further mapped to the region extending from nt 3575 to 5310 (R8) by introducing portions of the N-terminal half of ORF B from CHV1-EP713 into a CHV1-Euro7 background. A similar operation for the region extending from nt 2363 to 3575 (R7) eliminated the CHV1-EP713 p48 coding region as a major contributor to the severe colony morphology. Thus, differences in the mild and severe colony morphology mapped predominantly to a region extending from position 3575 through position 9879, with clear indications of multiple discrete determinants.

Use of the chimeras to map differences in canker morphology also exposed multiple determinants but was more revealing in that it was possible to uncouple several severe phenotypic traits. Isolates infected with all chimeras except R13 produced smaller cankers than that produced by CHV1-Euro7-infected isolates (Table 2). Thus, as observed for colony morphology, the CHV1-EP713 trait of small canker size is dominant and appears to be caused by multiple independent determinants within ORF B. In contrast, it was possible to map the difference in stromal pustule formation to the N-terminal portion of ORF B, i.e., upstream of the *Nar*I site, and to uncouple suppression of pustule formation from small canker size. This is particularly evident in the enlarged version of cankers produced by isolates infected with reciprocal chimeras R12 and R6 (shown at the bottom of Fig. 4). A characteristic CHV1-EP713 type of canker was observed when the region extending from nt 2363 to 5310 was derived from CHV1-EP713 (R12 or R5), while a small version of a CHV1-Euro7 canker, including the production of a significant level of pustules and the characteristic raised canker margins, was formed when this region was derived from CHV1-Euro7 (R6 or R10). Within this region, the CHV1-EP713 p48 coding domain is clearly the predominant contributor to suppression of pustule formation: introduction of the region extending from nt 2363 to 3575 into a CHV1-Euro7 background, R7, resulted in a significant (ca. eightfold) reduction in pustule formation. However, p48-mediated suppression of pustule formation appears to be dependent on proteins encoded within the CHV1-EP713 region from

nt 3575 to 5310, as evidenced by the increased level of pustule formation observed upon replacement with the CHV1-Euro7 counterpart in chimera R9. It is clear from the combined results that multiple viral domains contribute to differences in the severe and mild phenotypes and that different sets of determinants contribute to canker and colony morphologies. Although the present study provides a firm foundation for future refined mapping and mechanistic studies, additional detailed information concerning ORF B polyprotein processing will be required for a clear understanding of the phenotypic contributions of processing intermediates and/or viral protein-protein interactions.

The ability to uncouple small canker size from suppression of the formation of spore-producing pustules has implications for enhancing biological control potential. As discussed by MacDonald and Fulbright (21), successful hypovirulence-mediated biological control is likely to require a balance between ecological fitness and virulence attenuation. In order to persist and spread, a hypovirulent isolate must be able to effectively colonize and produce spores on chestnut bark. However, the ability to colonize must be tempered with a reduced capacity for canker expansion. The small canker and dense pustule production phenotype exhibited by isolates infected with chimeras R6, R10, R8, or R9 would appear to meet these criteria. The ability to construct transgenic hypovirulent *C. parasitica* strains containing nuclear copies of infectious hypovirus cDNA (9) provides the opportunity to combine these phenotypic improvements with a novel mode of virus transmission to ascospore progeny.

Several lines of evidence suggest that hypoviruses reduce virulence and induce other fungal phenotypic changes by altering cellular regulatory pathways, principally G protein-linked cyclic-AMP-mediated signal transduction (7, 10, 12). It has been proposed that these alterations compromise the ability of the invading fungus to respond appropriately to molecular and environmental cues during the infection process, thereby impeding penetration and canker expansion (23). It would follow from this model that the difference in canker morphology observed for isolates infected with the mild and severe hypovirus strains might result from differences in the degree to which the two viruses impact cellular signal transduction. It is anticipated that the mapping of domains responsible for the differences in symptoms exhibited by the two viruses will likely lead to the identification of viral determinants responsible for altering specific cellular signaling pathways. Preliminary results using pathway-specific promoter-reporter transformation plasmid constructs indicate that the chimeras can be used to correlate virus-induced changes in cellular signaling with virus-induced alterations in fungus-host pathogenic interactions (T. Parsley, L. M. Geletka, B. Chen, and D. L. Nuss, unpublished results). One could easily imagine how the resulting information could be exploited to design new strategies for manipulating fungal phenotype.

ACKNOWLEDGMENTS

This work was supported by NIH grant GM55981 to D.L.N.

We are grateful to Angus Dawe, Todd Parsley, and Gert Segers for helpful discussions.

REFERENCES

1. **Anagnostakis, S. L.** 1982. Biological control of chestnut blight. Science **215:** 466–471.
2. **Anagnostakis, S. L., and P. R. Day.** 1979. Hypovirulence conversion in *Endothia parasitica*. Phytopathology **69:**1226–1229.
3. **Bissegger, M., D. Rigling, and U. Heiniger.** 1997. Population structure and disease development of *Cryphonectria parasitica* in European chestnut forests in the presence of natural hypovirulence. Phytopathology **87:**50–59.
4. **Brandy, B. P., and S. M. Tavantzis.** 1990. Effect of hypovirulent *Rhizoctonia solani* on rhizoctonia disease, growth, and development. Am. Potato J. **67:** 189–199.
5. **Chen, B., G. H. Choi, and D. L. Nuss.** 1993. Mitotic stability and nuclear inheritance of integrated viral cDNA in engineered hypovirulence strains of the chestnut blight fungus. EMBO J. **12:**2991–2998.
6. **Chen, B., G. H. Choi, and D. L. Nuss.** 1994. Attenuation of fungal virulence by synthetic infectious hypovirus transcripts. Science **264:**1762–1764.
7. **Chen, B., S. Gao, G. H. Choi, and D. L. Nuss.** 1996. Extensive alteration of fungal gene transcript accumulation and elevation of G-protein-regulated cAMP levels by a virulence-attenuating hypovirus. Proc. Natl. Acad. Sci. USA **93:**7996–8000.
8. **Chen, B., and D. L. Nuss.** 1999. Infectious cDNA clone of hypovirus CHV1-Euro7: a comparative virology approach to investigate virus-mediated hypovirulence of the chestnut blight fungus *Cryphonectria parasitica*. J. Virol. **73:** 985–992.
9. **Choi, G. H., and D. L. Nuss.** 1992. Hypovirulence of chestnut blight fungus conferred by an infectious viral cDNA. Science **257:**800–803.
10. **Choi, G. H., B. Chen, and D. L. Nuss.** 1995. Virus-mediated or transgenic suppression of a G protein α subunit and attenuation of fungal virulence. Proc. Natl. Acad. Sci. USA **92:**305–309.
11. **Duffy, B. K., and D. M. Weller.** 1996. Biological control of take-all of wheat in the pacific northwest of the USA using hypovirulent *Gaeumannomyces graminis* var. *tritici* and fluorescent pseudomonads. J. Phytopathol. **144:**585–590.
12. **Gao, S., and D. L. Nuss.** 1996. Distinct roles for two G-protein α subunits in fungal virulence, morphology and reproduction revealed by targeted gene disruption. Proc. Natl. Acad. Sci. USA **93:**14122–14127.
13. **Heiniger, U., and D. Rigling.** 1994. Biological control of chestnut blight in Europe. Annu. Rev. Phytopathol. **32:**581–599.
14. **Hillman, B. I., R. Shapira, and D. L. Nuss.** 1990. Hypovirulence-associated suppression of host functions in *Cryphonectria parasitica* can be partially relieved by high light intensity. Phytopathology **80:**950–956.
15. **Hillman, B. I., D. W. Fulbright, D. L. Nuss, and N. K. Van Alfen.** 1995. Hypoviridae, p. 261–264. *In* F. A. Murphy, C. M. Fauquet, D. H. L. Bishop, S. A. Ghabrial, A. W. Jarvis, G. P. Martelli, M. A. Mayo, and M. D. Summers (ed.), Virus taxonomy. Springer-Verlag, New York, N.Y.
16. **Jaynes, R. A., and J. E. Elliston.** 1980. Pathogenicity and canker control by mixtures of hypovirulent strains of *Endothia parasitica* in American Chestnut. Phytopathology **70:**453–456.
17. **Ichielevich-Auster, M., B. Sneh, Y. Koltin, and I. Barash.** 1985. Suppression of damping-off caused by *Rhizoctonia* species by a nonpathogenic isolate of *R. solani*. Phytopathology **75:**1080–1084.
18. **Kasahara, S., and D. L. Nuss.** 1997. Targeted disruption of a fungal G-protein β subunit gene results in increased growth but reduced virulence. Mol. Plant-Microbe Interact. **8:**984–993.
19. **Kasahara, S., and D. L. Nuss.** 2000. Identification of *bdm-1*, a gene involved in G protein β-subunit function and α-subunit accumulation. Proc. Natl. Acad. Sci. USA **97:**412–417.
20. **Koonin, E. V., G. H. Choi, D. L. Nuss, R. Shapira, and J. D. Carrington.** 1991. Evidence for common ancestry of a chestnut blight hypovirulence-associated double-stranded RNA and a group of positive-strand RNA plant viruses. Proc. Natl. Acad. Sci. USA **88:**10647–10651.
21. **MacDonald, W. L., and D. W. Fulbright.** 1991. Biological control of chestnut blight: use and limitation of transmissible hypovirulence. Plant Dis. **75:** 656–661.
22. **Melzer, M., and G. J. Boland.** 1995. Transmissible hypovirulence in *Sclerotinia minor*. Can. J. Plant. Pathol. **18:**19–28.
23. **Nuss, D. L.** 1996. Using hypoviruses to probe and perturb signal transduction processes underlying fungal pathogenesis. Plant Cell **8:**1845–1853.
24. **Puhalla, J. E., and S. L. Anagnostakis.** 1971. Genetics and nutritional requirements of *Endothia parasitica*. Phytopathology **61:**169–173.
25. **Shapira, R., G. H. Choi, and D. L. Nuss.** 1991. Virus-like genetic organization and expression strategy for a double-stranded RNA genetic element associated with biological control of chestnut blight. EMBO J. **10:**731–739.
26. **Shapira, R., G. H. Choi, B. I. Hillman, and D. L. Nuss.** 1991. The contribution of defective RNAs to complexity of viral-encoded double-stranded RNA populations present in hypovirulent strains of the chestnut blight fungus, *Cryphonectria parasitica*. EMBO J. **10:**741–746.
27. **Shapira, R., and D. L. Nuss.** 1991. Gene expression by a hypovirulence-associated virus of the chestnut blight fungus involves two papain-like protease activities. J. Biol. Chem. **266:**19419–19425.
28. **Zhou, T., and G. J. Boland.** 1998. Suppression of dollar spot by hypovirulent isolates of *Sclerotinia homoeocarpa*. Phytopathology **88:**788–794.